



HAL
open science

Seaweed consumption in France: Key data for exposure and risk assessment

Anne-Sophie Ficheux, Ophélie Pierre, Raphaële Le Garrec, Alain-Claude Roudot

► **To cite this version:**

Anne-Sophie Ficheux, Ophélie Pierre, Raphaële Le Garrec, Alain-Claude Roudot. Seaweed consumption in France: Key data for exposure and risk assessment. *Food and Chemical Toxicology*, 2022, 159 (5), pp.112757. 10.1016/j.fct.2021.112757 . hal-04343400

HAL Id: hal-04343400

<https://hal.science/hal-04343400>

Submitted on 22 Jul 2024

HAL is a multi-disciplinary open access archive for the deposit and dissemination of scientific research documents, whether they are published or not. The documents may come from teaching and research institutions in France or abroad, or from public or private research centers.

L'archive ouverte pluridisciplinaire **HAL**, est destinée au dépôt et à la diffusion de documents scientifiques de niveau recherche, publiés ou non, émanant des établissements d'enseignement et de recherche français ou étrangers, des laboratoires publics ou privés.



Distributed under a Creative Commons Attribution - NonCommercial 4.0 International License

Seaweed consumption in France: key data for exposure and risk assessment

Authors: Ficheux Anne-Sophie¹, Pierre Ophélie¹, Le Garrec Raphaële¹, Roudot Alain-Claude¹

¹ University of Brest, LIEN, Brest, France

Corresponding author: Anne-Sophie Ficheux

E-mail : anne-sophie.ficheux@univ-brest.fr

Keywords: seaweeds – food – consumption – enquiry – exposure and risk assessment

Word count : 5687

1 **A novel benzotriazole derivate with Twisted Intramolecular**
2 **Charge Transfer and Aggregation Induced Emission**
3 **features for proton determination**

4 Shaoheng Li ^a, Na Shi ^b, Mingyu Zhang ^a, Zhaokang Chen ^a, Daichuan Xia ^a, Qingchuan Zheng ^b,

5 Guodong Feng^{*a} and Zhiguang Song^{*a}

6
7 ^a College of Chemistry, Jilin University, Changchun, Jilin, 130021, China.

8 ^b Institute of Theoretical Chemistry, College of Chemistry, Jilin University,
9 Changchun, Jilin, 130023, China.

10
11
12 *Corresponding authors. E-mail addresses: fenggd@jlu.edu.cn (G. D. Feng), E-mail address:
13 szg@jlu.edu.cn (Z. G. Song)

14
15 **Abstract:**

16 Molecules with Aggregation-Induced Emission (AIE) effects could show strong
17 emission in solid or aggregate form, thus they are suitable for applications in the field
18 of solid luminescent materials. **According to former** reporting, AIE molecules are
19 always J-aggregates. In this study, a new benzotriazole derivate with electron donor-
20 acceptor structure was synthesized. (E)-4-(2-(1H-benzo[d][1,2,3] triazol-1-yl) vinyl)-
21 N, N-dimethylaniline (BTADA) has both TICT and AIE effect, even though it is H-
22 aggregate. Furthermore, BTADA could **respond** to proton in solution and solid form.
23 Due to its multiple binding sites, proton would bind to benzotriazole and
24 dimethylaniline moiety successively when BTADA was exposed to acid, and the

25 fluorescent color changed from green to yellow then blue as the concentration of
26 proton increased. Such phenomena indicate BTADA has potential usage in proton
27 detection.

28

29 **Keywords** Benzotriazole, H-aggregate, Aggregation-Induced Emission, Proton Response,
30 Twisted Intramolecular Charge Transfer

31

32 **1. Introduction**

33 Normally, chromophoric organic dyes with planar structure always show strong
34 luminescence **properties** in dispersed states, but the fluorescence will be **dramatically**
35 quenched in solid or aggregate states because the energy from excited states can decay
36 back via non-radioactive channels like π - π stacking interactions between molecules
37 [1], known as **Aggregation-Caused Quenching** (ACQ) [2, 3]. Compared with ACQ
38 molecules, molecules with Aggregation-Induced Emission (AIE) effects could show
39 strong fluorescence emission in solid or aggregate form. This effect was first brought
40 by the group of Tang in 2001 [4], and has gained pile of attention since day one. Small
41 organic molecules with AIE effect have stood out of the line due to the obvious
42 advantages in some application fields. AIE molecules are suitable for applications in
43 the field of solid luminescent materials because the luminescent molecules are
44 required to be in a tightly packed aggregate or solid state [5, 6] rather than in a
45 dispersed state in practical applications. **In the field of fluorescence analysis, the**

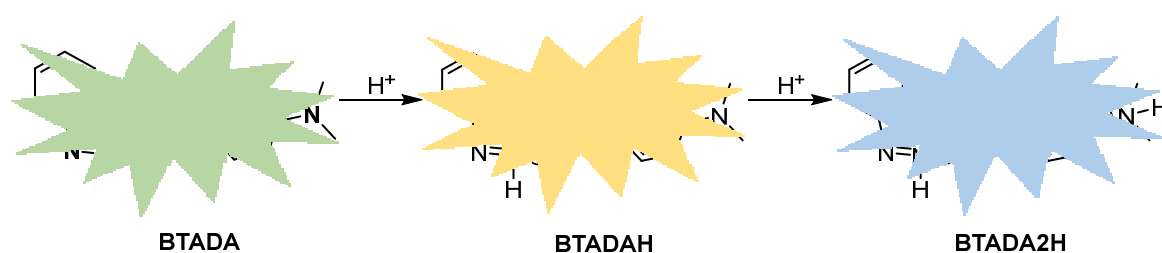
46 ability of fluorescent probes to detect analytes in high water content systems is
47 sometimes required. Because of hydrophobicity, the organic fluorescent molecules
48 usually form aggregates in water. Traditional organic dyes suffer from ACQ effect and
49 are restricted from application. However, AIE-based probes could be easily
50 engineered and possess high photobleaching resistance. This kind probes can keep
51 high sensitivity and selectivity to detect analytes in aqueous solution. Nowadays,
52 these AIE organic molecules have been widely used in Organic Light-Emitting Diodes
53 (OLEDs) [7 - 9], biosensor (for proteins [10 - 11], DNAs [12 - 14], amino acids [15 -
54 17], and so on), chemosensor (for ions [18], gases [19], explosives [20 - 21] and so
55 on) and other varies fields.

56 Many fluorescence molecules have an electron donor-acceptor (D-A) structure. In
57 some cases, there is a bridge that link the electron donor part and the electron acceptor
58 part in fluorescence molecules. When the external conditions change, such as
59 temperature, pressure and polarity of the solvent, these molecules will twist as well.
60 This kind of torsion leads to a charge separation among the whole molecule, narrows
61 the band gap and results in red shift emission. This phenomenon is called “Twisted
62 intramolecular charge transfer” (TICT) [22]. TICT effect of organic compounds have
63 been systematically studied [23 - 25] and always used to detect some target molecules
64 in analytical fields [26 - 28]. In recent years, organic fluorescence molecules with
65 both TICT and AIE effects have attracted extensive attention and been applied in
66 many analytical fields. Some of these TICT-AIE organic molecules like

67 tetraphenylethene (TPE) derivatives [29], boron dipyrromethene (BODIPY)
68 derivatives [30], cyan derivatives [31 - 33] and 9,10-Bis[4'-(4''-aminostyryl) styryl]
69 anthracene derivatives [34] are J-aggregates when they generate AIE effect. **This**
70 means they tend to pack in a “head-to-toe” form when these molecules aggregate. J-
71 aggregates of AIE fluorescence molecules share as following characteristics: small
72 Stokes-shift with a narrow band gap and a bathochromic shift of emission wavelength
73 [35]. However, there’s another type of aggregation **in** which the molecules are packed
74 “face-to-face”. Apart from J-aggregates, this kind of aggregation with a hypsochromic
75 shift, is normally called “H-aggregate” [36 - 37]. H-aggregates have longer Stokes-
76 shift than J-aggregates. Meanwhile, the UV-vis absorb and fluorescence emission
77 spectra in aggregated states are blue shifted compared with those in dispersed states
78 [35]. But, there are only a few reports about H-aggregate molecules in AIE
79 luminogens. For example, Distyrylbenzene (DSB) [38] is a classic H-type AIE
80 luminogens. Other examples include merocyanine and other dyes **containing**
81 heteroaromatic rings [39 - 40]. However, it **comes** to our notice that benzotriazole
82 derivatives as AIE fluorescence molecules are lack study. We **hereby reported** a new
83 type of benzotriazole derivative that shows AIE effect while **aggregating** in the H-
84 type.

85 Benzotriazole, compare to other heteroaromatic compounds, exhibits stronger
86 aromaticity, flatter planarity, and can act like a much stronger electron-acceptor [41].
87 **Naturally**, benzotriazole can play an important role among fluorescence organic

88 molecules. However, correlational research work is rarely reported. In this work, we
89 synthesize (E)-4-(2-(1H-benzo[d][1,2,3] triazol-1-yl) vinyl)-N, N-dimethylaniline
90 (BTADA). Due to its wide π conjunction and electron donor-acceptor construct,
91 BTADA should exhibit high fluorescence emission in solution system. Following
92 experiments **confirmed our conjecture**. Moreover, further experiments indicate other
93 unexpected properties. In addition to exhibiting different fluorescence emission
94 wavelength in **various** solvent, BTADA has strong fluorescence emissive activity in
95 solid form. **The single-crystal structure of BTADA clearly shows that BTADA is a**
96 **classic H-aggregate**. As discussed above, AIE property of benzotriazole derivative is
97 rarely seen in H-aggregates. More to that, with the strong electron donor-acceptor
98 structure of BTADA, the benzotriazole part and dimethylamine part are both rotors
99 that can spin over the covalent bond on both sides of alkene bridge. Which makes it a
100 classic TICT molecule. To summarize, during the aggregation of monomer, the
101 BTADA shows TICT-AIE effect. Even more to the point, BTADA exhibited a dual-
102 step response to proton, which means it has a potential application in proton detection.



104 **Scheme 1.** Schematic diagram of proton response of BTADA

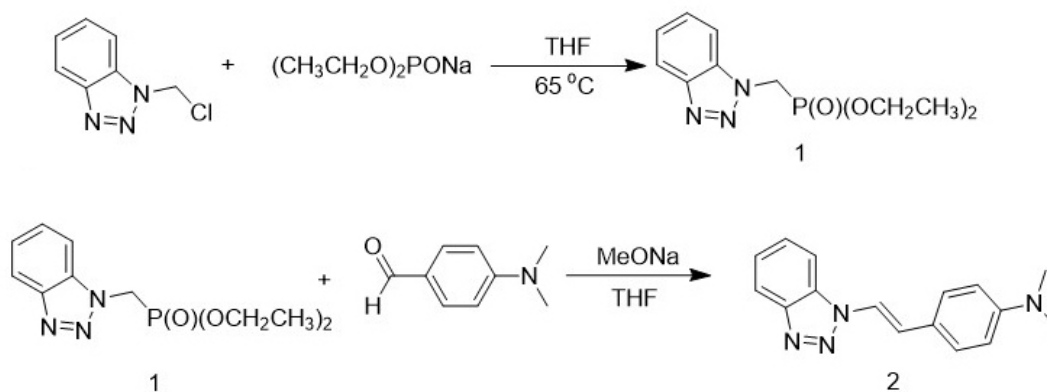
105 **2. Experimental section**

106 *2.1. Materials and measurements*

107 All the raw materials were obtained from commercial supplies and used without
108 further purification. THF were dehydrated by reflux with solid Na. Water used
109 throughout all experiments was purified with Millipore system. ^1H NMR and ^{13}C
110 NMR spectra were recorded on Bruker 400 NMR spectrometer. Chemical shifts are
111 reported in ppm with TMS as reference. Mass spectra were obtained with Agilent1290
112 - Bruker microTOF QII mass spectrometer. The UV-vis absorption spectra were
113 obtained using a Shimadzu UV-3100 Spectrophotometer. Fluorescence data was
114 measured on a Hitachi F-2700 Fluor spectrophotometer.

115 The single crystal of BTADA was obtained from saturated dichloromethane
116 solution by slow evaporation at room temperature. The crystallographic data for
117 BTADA was collected on a Siemens Smart CCD diffractometer with graphite-
118 monochromated Mo-K α ($\lambda = 0.71073 \text{ \AA}$) radiation at room temperature. The structure
119 was solved by direct methods with SHELXT1 and refined by full-matrix least-squares
120 on F^2 using the SHELXTL-20142. All non-hydrogen atoms were refined with
121 anisotropic displacement parameters. The hydrogen atoms of the ligands were
122 generated geometrically.

123 2.2. Synthesis of BTADA



124

1

2

125

Scheme 2. Synthesis route of BTADA

126

127 *2.2.1. Synthesis of Diethyl ((1H-benzo[d] [1,2,3] triazol-1-yl) methyl) phosphonate*

128 (1)

129 Diethyl ((1H-benzo[d] [1,2,3] triazol-1-yl) methyl) phosphonate (**1**) was
 130 synthesized according to literature [42].

131 *2.2.2. Synthesis of BTADA*

132 MeONa (1.08 g, 20 mmol) and **1** (5.38 g, 20 mmol) was added to dry THF (20 ml)
 133 under N_2 , stirred at $0\text{ }^\circ\text{C}$ for 30 minutes. After which the mixture of
 134 4-Dimethylaminobenzaldehyde (1.49 g, 10 mmol) and THF (5ml) was slowly added
 135 to the reaction solution with syringe. The reaction temperature was then heated to
 136 reflux. After stirred for 12h under the protection of N_2 , the reaction was quenched by
 137 water. The aqueous solution was extracted with dichloromethane (3*20ml) and the
 138 combined organic phase was dried by Na_2SO_4 . The solvent was removed by vacuum
 139 evaporation. The crude product was purified by a silica gel column with ethyl acetate
 140 and petroleum ether (1:5) as eluent, the products was obtained as yellow crystal in a

141 yield of 90 % (2.38 g). ¹H NMR (400 MHz, Chloroform-*d*): δ 8.10 (d, *J* = 8.3 Hz,
142 1H), 7.82 – 7.71 (m, 2H), 7.56 (ddd, *J* = 8.1, 6.9, 1.0 Hz, 1H), 7.48 – 7.35 (m, 4H),
143 6.79 – 6.72 (m, 2H), 3.02 (s, 6H). ¹³C NMR (101 MHz, Chloroform-*d*): δ 150.62,
144 146.26, 131.52, 127.86, 127.77, 124.38, 122.34, 122.07, 120.31, 118.14, 112.42,
145 110.23, 40.38. HRMS: *m/z* 265.1390 [(M+H)⁺, calcd 265.1409].

146 *2.3 fluorescence experiment*

147 The concentration of BTADA was 1×10^{-5} mol L⁻¹, excitation wavelength was 365
148 nm, excitation and emission slit were both 5 nm.

149 *2.3.1 fluorescence response to different solvent*

150 BTADA was respectively dissolved in CH₂Cl₂, CHCl₃, DMF, THF, Acetone,
151 CH₃CN, ethanol, ethyl acetate, toluene and cyclohexene. The final concentration of
152 BTADA was 1×10^{-5} mol L⁻¹.

153 *2.3.2 fluorescence response to the water fraction of the solvent*

154 BTADA was dissolved in methanol, the concentration of BTADA was 2×10^{-4} mol
155 L⁻¹. Then 100 μL of BTADA **solution** was diluted with the mixture of methanol and
156 water to 2 mL.

157 *2.3.3 fluorescence response to the **viscosity** of the solvent*

158 BTADA was dissolved in methanol, the concentration of BTADA was 2×10^{-4} mol
159 L⁻¹. Then 100 μL of BTADA **solution** was diluted with the mixture of methanol and
160 glycerol to 2 mL.

161 *2.3.4 fluorescence response to proton*

162 BTADA was dissolved in CHCl_3 , the concentration of BTADA was $2 \times 10^{-4} \text{ mol L}^{-1}$
163 ¹. After different volume of trifluoroacetic acid (TFA, $2.5 \times 10^{-3} \text{ mol L}^{-1}$) was added
164 into BTADA solution, the mixed solution was diluted with CHCl_3 to 2 mL.

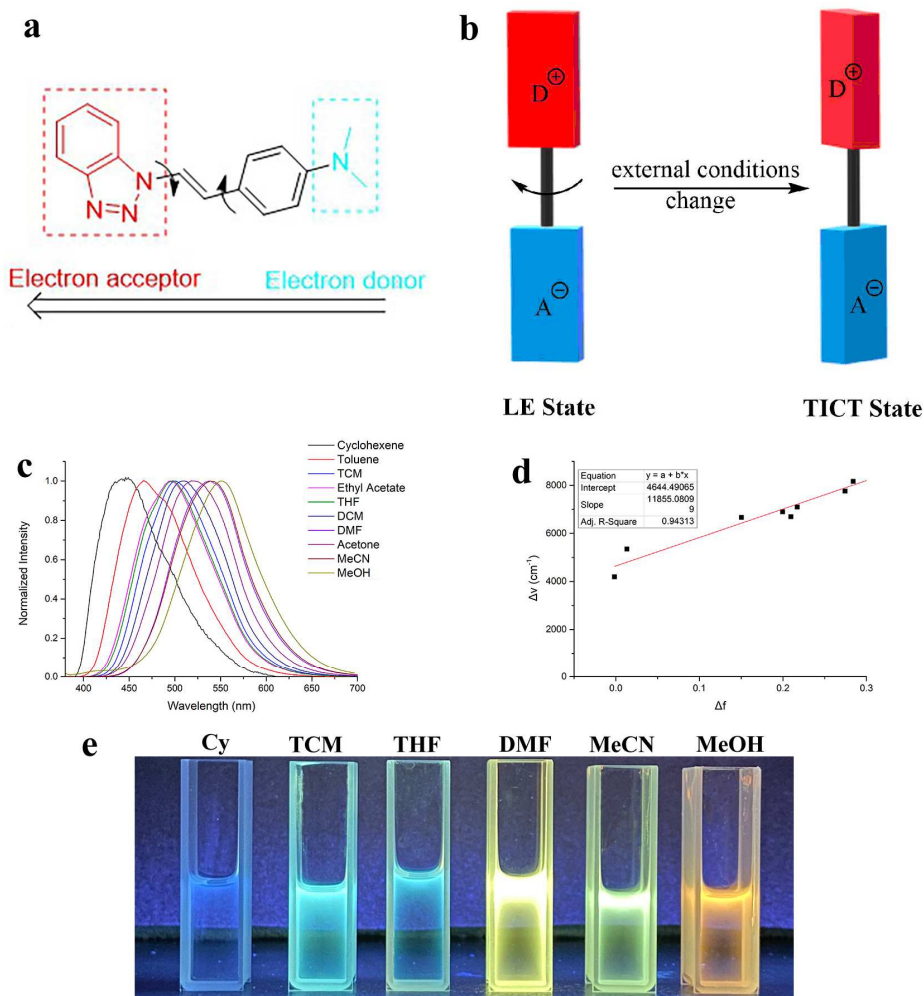
165 3. Results and discussion

166 3.1 Twisted intramolecular charge transfer

167 BTADA was synthesized through the above reaction procedures as yellow platy
168 crystal. The total yield was 81%. As shown in Fig. 1a, BTADA contains a classic
169 electron donor-acceptor structure. The N, N-dimethylamine part (electron donor) and
170 the benzotriazole part (electron acceptor) in BTADA are connected through a
171 conjugated π -bridge. The existence of rotatable C-C and C-N δ bond on both sides of
172 alkene bridge make them rotors. Meanwhile, the density functional theory (DFT) was
173 used to calculate the charge distribution in BTADA. The results are shown in Fig. S3.
174 In the highest occupied molecular orbital (HOMO) of BTADA, most of the electron
175 density is on the N, N-dimethylamine part (electron donor), while in the lowest
176 unoccupied molecular orbital (LUMO) of BTADA, most of the electron density is on
177 the benzotriazole part (electron acceptor).

178 Generally, fluorophores comprise D- π -A conjugated structures that usually form
179 TICT states upon light irradiation. BTADA as a D- π -A structure molecule has two
180 kinds of excited states, locally excited (LE) state and TICT state (Fig. 1b). Through
181 the effect of external conditions, LE state and TICT state can be easily transformed
182 into each other. When dissolved in low-polar solvent, BTADA is in a coplanar

183 conformation and the LE state is **the** lowest-energy state. As shown in Fig. 1c, the
184 cyclohexane solution of BTADA was observed a strong fluorescence emission
185 wavelength at 449 nm when the excited wavelength is 365 nm. **With the increase of**
186 **the polarity of the solvent**, the multiple interactions between the electron donor and
187 acceptor parts of BTADA can enhance the HOMO level and reduce the LOMO level
188 resulting in a TICT state. **Meanwhile, the fluorescence emission of BTADA has an**
189 **obvious bathochromic-shift as the polarity of solution increases and BTADA**
190 **displayed different fluorescene colors from blue to orange in different polarity**
191 **solvents.** (Fig. 1c and 1e). As shown in Fig. 1d, the polar function (Δf) of solvents
192 and the Stokes shift ($\Delta \nu$) shows ideal linear relationships and fitted well with the
193 Lippert–Mataga plot [43]. These experimental results confirm the TICT property of
194 BTADA by the solvent polarity dependent fluorescent emission [44].



195

196 **Fig. 1.** (a). Electron structure of BTADA; (b). LE state and TICT state of BTADA; (c).

197 Fluorescence photographs of BTADA in different solvent; (d). Plot of the Stokes shift of

198 BTADA in each solvent versus Δf of the respective solvent. The concentrations of BTADA in

199 the experiments are 50 μM ; (e). Fluorescence images of BTADA in different solvent

200 3.2 Aggregation-induced emission effect of BTADA

201 In this part, the fluorescence emission behaviors of BTADA in H_2O -MeOH solution

202 with different water contents (f_w , the volume percentage of water in H_2O -MeOH

203 solution) were studied. As shown in Fig. 2a and 2b, the yellow fluorescence (550 nm)

204 can be observed under 365 nm as excitation wavelength when BTADA is dissolved in

205 pure ethanol. The fluorescence of BTADA is slightly bathochromic-shift and
206 gradually weakens. When water contents are increased from 0 to 70 % in H₂O-MeOH
207 solution, which is a sign that the BTADA molecule has turned into a TICT state.
208 While the f_w is over 70%, the fluorescence emission intensity is dramatically
209 increased and fluorescence emission wavelength has obviously blue-shifted into 507
210 nm under 365 nm as excitation wavelength. In this stage, BTADA molecules are easy
211 to aggregate due to the hydrophobic interaction. Such aggregation will lead to the
212 restriction of intramolecular rotations (RIR), thus the non-radioactive channel for
213 excited state to decay back to ground state are cut off, resulting in Aggregation-
214 Induced Emission [45]. To further explain the mechanism of the BTADA molecules'
215 AIE effect, photophysical behaviors of BTADA were studied in the system of
216 methanol-glycerol mixture as well (Fig. 2c). When the volume percentage of glycerol
217 in glycerol-MeOH solution (f_g) is increased, the viscosity of methanol-glycerol
218 mixture solution goes up, and so does the fluorescence intensity of BTADA. It
219 indicates that BTADA is harder and harder to rotate when the viscosity of solution is
220 gradually increased. This also proves the RIR is the reason for the AIE effect of
221 BTADA.